Local Alignment Search Tool (BLAST) searches: LST-2 (R160.7) = XM 035371.4 and a set of related sequences, LST-3 (Y37A1B.1) = AK023438 and a set of related sequences, LST-4 (Y37A1B.2) = sorting nexin 9/18, and DPY-23 (R160.1) = μ subunit of the Clathrin Adaptor Protein Complex 2. Recent biochemical data for the orthologs of DPY-23 and LST-4 in cultured cells have suggested roles for them in the degradation of EGFR (*21*, *22*); for these genes, our *C. elegans* data provide evidence for their roles as negative regulators of EGFR activity in vivo. The mammalian orthologs of LST-2 and LST-3 have not been previously implicated in negative regulation of EGFR-MAPK signaling. Analysis of potential functional domains with the Simple Modular Architecture Research Tool (SMART) (*23*) reveals that LST-2 contains a FYVE domain, a membrane targeting domain that binds specifically to a phospholipid that resides mainly in endosomal membranes (*24*), and therefore may influence the endocytic trafficking of LET-23 or the subcellular localization of other components of the EGFR-MAPK pathway. LST-3 contains SAF-A/B, Acinus, and PIAS (SAP) domains, a motif found in DNA binding proteins, and thus does not suggest a potential direct role in modulating EGFR-MAPK activity. LST-1 (T22A3.3) does not have a recognizable mammalian ortholog; it was found in a genome-wide yeast two-hybrid screen for proteins that interact with the MAPK ortholog MPK-1 (*25*) and hence may act directly on MAP kinase.

14. T. Berset, E. F. Hoier, G. Battu, S. Canevascini, A. Hajnal, *Science* **291**, 1055 (2001).
15. Most of the *lst* gene transcriptional reporters were made by a polymerase chain reaction fusion protocol (*26*), and extrachromosomal arrays were generated in a *pha-1(e2123ts)* background, using *pha-1(+)* as a transformation marker (*27*). For extrachromosomal arrays, more than one line was scored as indicated, and we mitigated against the potential lack of expression in P5.p or P7.p due to mosaicism by including data only for animals in which expression (even if faint) could be seen in P3.p, P4.p, and P8.p, or for both P5.p and P7.p. The exception to these general procedures was *lst-1*, for which conventional constructs and integrated transgenes were used. For transgene details, see (*9*).
16. G. J. Beitel, S. Tuck, I. Greenwald, H. R. Horvitz, *Genes Dev.* **9**, 3149 (1995).
17. P. Heitzler, P. Simpson, *Development* **117**, 1113 (1993).
18. T. L. Jacobsen, K. Brennan, A. M. Arias, M. A. Muskavitch, *Development* **125**, 4531 (1998).
19. D. D. Shaye, I. Greenwald, *Nature* **420**, 686 (2002).
20. I. Maillard, W. S. Pear, *Cancer Cell* **3**, 203 (2003).
21. Q. Lin, C. G. Lo, R. A. Cerione, W. Yang, *J. Biol. Chem.* **277**, 10134 (2002).
22. I. Rapoport *et al.*, *EMBO J.* **16**, 2240 (1997).
23. I. Letunic *et al.*, *Nucleic Acids Res.* **30**, 242 (2002).
24. M. A. Lemmon, *Traffic* **4**, 201 (2003).
25. A. J. Walhout *et al.*, *Science* **287**, 116 (2000).
26. O. Hobert, *Biotechniques* **32**, 728 (2002).
27. M. Granato, H. Schnabel, R. Schnabel, *Nucleic Acids Res.* **22**, 1762 (1994).
28. G. Garriga, personal communication.
29. L. Timmons, A. Fire, *Nature* **395**, 854 (1998).
30. WormBase: The Biology and Genome of *C. elegans*, www.wormbase.org.

31. We thank A. Wong for initial and encouraging computational analyses to identify potential LIN-12 targets, H. Yu for collaborating on the development of Cluster Analyzer for Transcription Sites (CATS), and X. Zhou for generating transgenic lines. We thank the Caenorhabditis Genetic Center for strains, Y. Kohara for cosmids, and A. Fire and M. Vidal for plasmids. We appreciate the comments on the manuscript from O. Hobert, S. Jarriault, R. Mann, and D. Shaye. A.Y. was supported by a fellowship from the National Sciences and Engineering Research Council of Canada (NSERC) and in part by NIH CA095389 (to I.G.). C.B. is a postdoctoral associate and I.G. is an investigator of the Howard Hughes Medical Institute.

Supporting Online Material

www.sciencemag.org/cgi/content/full/303/5658/663/DC1
Materials and Methods
Fig. S1
References

18 September 2003; accepted 7 November 2003

Reactivation of the Paternal X Chromosome in Early Mouse Embryos

Winifred Mak,[1] Tatyana B. Nesterova,[1] Mariana de Napoles,[1] Ruth Appanah,[1] Shinya Yamanaka,[2] Arie P. Otte,[3] Neil Brockdorff[1]*

It is generally accepted that paternally imprinted X inactivation occurs exclusively in extraembryonic lineages of mouse embryos, whereas cells of the embryo proper, derived from the inner cell mass (ICM), undergo only random X inactivation. Here we show that imprinted X inactivation, in fact, occurs in all cells of early embryos and that the paternal X is then selectively reactivated in cells allocated to the ICM. This contrasts with more differentiated cell types where X inactivation is highly stable and generally irreversible. Our observations illustrate that an important component of genome plasticity in early development is the capacity to reverse heritable gene silencing decisions.

X inactivation is the developmentally regulated silencing of one of the two X chromosomes in female mammals, providing the mechanism for dosage compensation of X-linked genes relative to XY males. In mouse embryos, there is imprinted X inactivation of the paternal X chromosome (Xp) in the extraembryonic trophectoderm (TE) and primitive endoderm (PE). In all other cells, X inactivation is random. Establishment of these patterns has been thought to occur in a lineage-specific manner, with imprinted X inactivation initiated only in TE and PE cells as they differentiate at the blastocyst stage. In contrast, ICM cells, which give rise to the embryo proper, have been thought to retain both X chromosomes in the active state until they differentiate and undergo random X inactivation during early postimplantation development (*1*–*5*). Paradoxically, *Xist* RNA, the cis-acting signal that initiates X inactivation, is expressed from Xp as early as the two-cell stage (*6*, *7*). This has been rationalized by supposing that cells of the early embryo cannot respond to *Xist* RNA (*6*).

In a recent study, we have shown that recruitment of the Eed-Ezh2 Polycomb-Group (PcG) complex to the inactive X (Xi), is required to establish trimethylation of histone H3 lysine-27 (H3-K27) in postimplantation embryos (*8*). In the course of analyzing localization of Eed-Ezh2 on Xi in preimplantation embryos, we found that PcG localization occurs in all cells of early- and mid-stage XX blastocysts, including those corresponding morphologically to the ICM (Fig. 1A). In contrast, localization to Xi was no longer detectable in the ICM region of late-stage blastocysts, despite high levels of the Eed-Ezh2 proteins in the nuclei (Fig. 1B). Scoring data demonstrate that only early-stage blastocysts have Eed-Ezh2 foci in 100% of cells (Fig. 1C). In dual staining experiments, Ezh2 was seen to colocalize with Eed at all stages analyzed and Eed-Ezh2 foci colocalized with *Xist* RNA domains (fig. S1, A to C).

Eed-Ezh2 localization to Xi in the ICM was confirmed using dual staining for Eed and the recently described homeodomain protein Nanog, expressed specifically in ICM cells (*9*, *10*). Eed foci were detectable in all Nanog-positive cells in early- and mid-stage blastocysts (Fig. 1, D and E) but were progressively lost at later stages (Fig. 1F). Interestingly, loss of Eed foci in the ICM region of maturing blastocysts occurs specifically in Nanog-positive cells, representing precursors of the embryo proper, but does not occur in Nanog-negative cells, which represent the primitive endoderm lineage.

Our observations led us to consider that imprinted X inactivation may occur in all cells of early blastocysts and may then be selectively reversed in the ICM, establishing the ground state for subsequent random X inactivation. To determine whether early ICM cells exhibit other markers of X inactivation, we carried out dual labeling for Eed and specific modifications

[1]X inactivation group, MRC Clinical Sciences Centre, ICSM, Hammersmith Hospital, London, W12 0NN, UK. [2]Laboratory of Animal Molecular Technology, Research and Education Center for Genetic information, Nara Institute of Science and Technology, Nara 630-0192, Japan. [3]Swammerdam Institute of Life Sciences, University of Amsterdam, Plantage Muidergracht 12, 1018 TV Amsterdam, Netherlands.

*To whom correspondence should be addressed. E-mail: neil.brockdorff@csc.mrc.ac.uk

on histone N-termini, namely trimethylation of H3-K27, deacetylation of H3-K9, loss of methylation at H3-K4, and deacetylaton of H4 (*8*, *11*–*13*) (fig. S2, A to D).

Eed localization to Xi in XX embryos is first detectable in morula (*8*). At this stage, H3-K27 methylation on Xi was only detectable in some cells with Eed foci (Fig. 2, A, B, and D). The proportion increased rapidly thereafter, and by blastocyst stage H3-K27 methylation on Xi was detected in the majority of cells, including in the ICM region (Fig. 2, C and D). Hypoacetylation of H3-K9 and loss of H3-K4 methylation, which are early markers of X inactivation (*11*), were detectable in all cells with Eed localization to Xi, even at the morula stage (Fig. 2, E and F). Also, H4 hypoacetylation, a later marker for the X inactivation process (*8*, *11*, *13*), was seen underlying Eed foci at morula and subsequent stages (Fig. 2G). These results demonstrate that X inactivation initiates earlier than previously thought, at or even before morula stage, and that markers of X inactivation other than Eed-Ezh2 localization are established in ICM cells of early blastocysts.

Taken together, our results show that paternally imprinted X inactivation is established in all cells in early XX preimplantation embryos, implying that there is a subsequent reactivation event in cells of the ICM. Because Xp *Xist* expression is progressively extinguished in ICM cells during blastocyst maturation (*6*, *7*), we infer that this may be the mechanism of X reactivation. This contrasts with differentiated somatic cells in which maintenance of X inactivation is *Xist*-independent (*14*, *15*). Analysis of Eed-Ezh2 and H3-K27 methylation supports this interpretation. First, using immunoRNA-FISH (fluorescence in situ hybridization) analysis, we found that Eed-Ezh2 complexes dissociate rapidly from Xi as presumptive ICM cells begin to extinguish Xp *Xist* RNA expression (Fig. 3A). However, loss of tri-meH3-K27 staining on Xi disappeared more gradually. Thus, immunostaining for both Eed and meH3-K27 revealed cells in which Eed foci were lost, but meH3-K27 staining was still clearly detectable (Fig. 3B). In all instances, cells showing this pattern also had high overall levels of Eed staining in the nucleus, indicating that they

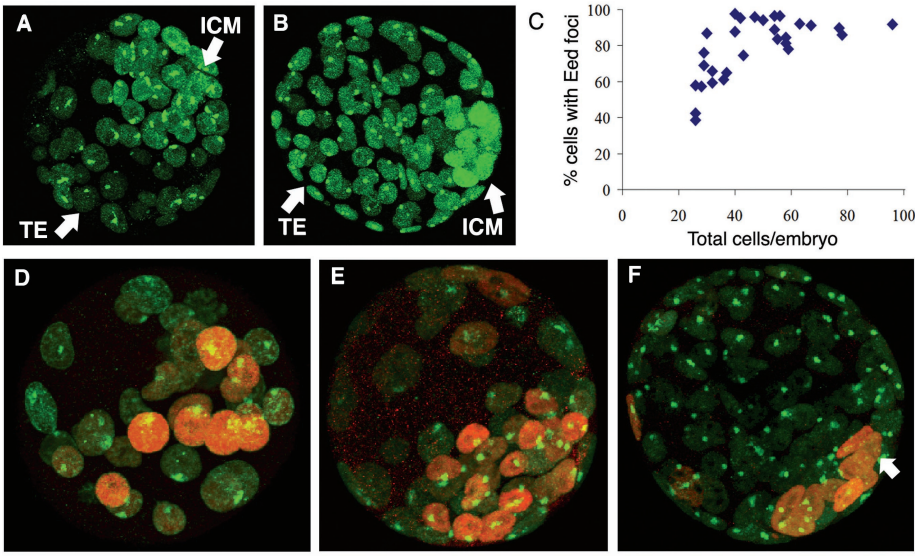

Fig. 1. Eed-Ezh2 localization in ICM cells. Combined optical sections through (**A**) early- and (**B**) late-stage XX blastocysts immunostained for Eed (green). Presumptive ICM and TE are indicated with arrows. (**C**) Scoring data illustrating the proportion of cells with Xi associated Eed foci in individual XX embryos between morula and late blastocyst. (**D** to **F**) Combined optical sections illustrating (D) early-, (E) mid- and (F) late-stage XX blastocysts stained for Eed (green) and Nanog (red). Arrow in (F) indicates Nanog-positive cells without Eed foci.

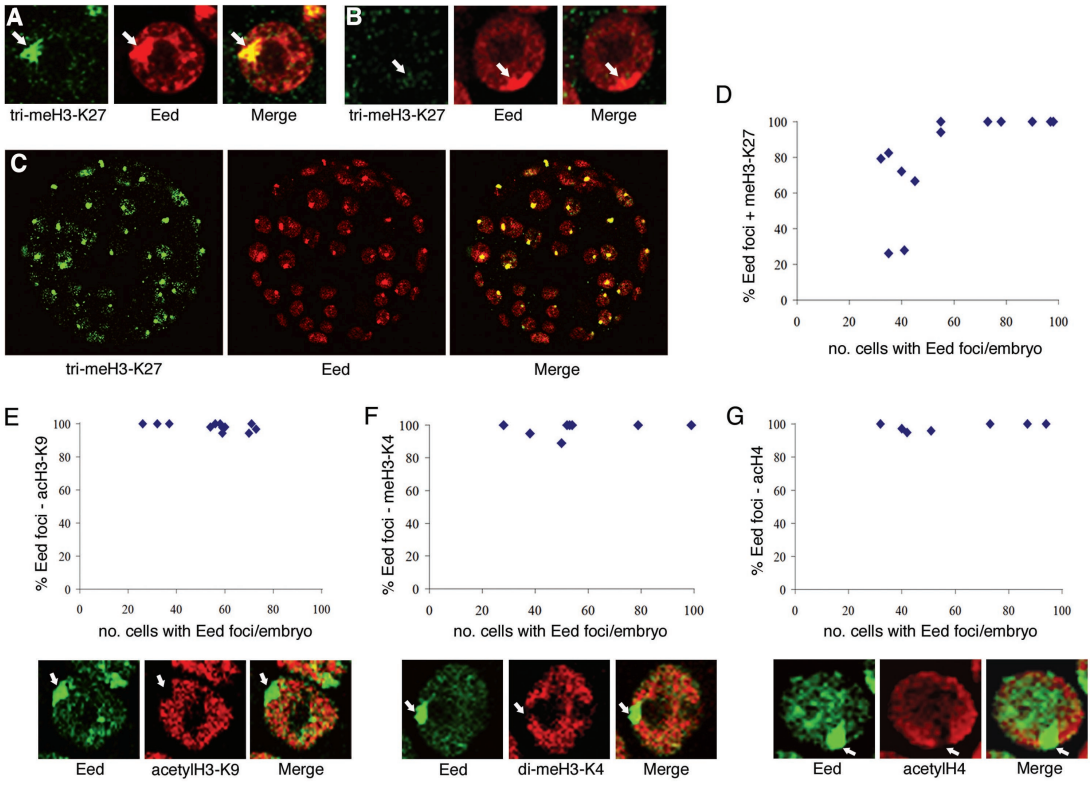

Fig. 2. Inactive X chromatin modification in early embryos. (**A** and **B**) Optical sections illustrating examples of cells in XX morula-stage embryos showing Eed (red) localization to Xi (arrows), either (A) with or (B) without associated tri-meH3-K27 (green). (**C**) Combined optical sections through a mid-stage XX blastocyst illustrating colocalization of Eed and tri-meH3-K27 in all cells. (**D**) Scoring data showing the proportion of Xi Eed foci with associated tri-meH3-K27 in individual XX embryos between morula and late blastocyst. (**E** to **G**) Scoring data for individual XX embryos between morula and late blastocyst stage, showing association of Xi Eed foci with hypoacetylation of (E) H3-K9, loss of dimethylation at (F) H3-K4, and (G) hypoacetylation of H4. Optical sections illustrating Eed (green) foci and absence of histone modification (red) are provided under each scatter plot.

represent ICM cells (Fig. 1B). In the ICM of mature blastocysts, both Eed and meH3-K27 staining of Xi were no longer detectable (Fig. 3C). At 5.5 days post coitum (dpc), as epiblast cells begin to undergo random X inactivation, localization of Eed-Ezh2 and associated tri-meH3-K27 were again detectable (Fig. 3D). This sequential loss and reestablishment—first of Eed-Ezh2 localization and then of tri-meH3-K27—provides a direct illustration of X reactivation in ICM cells.

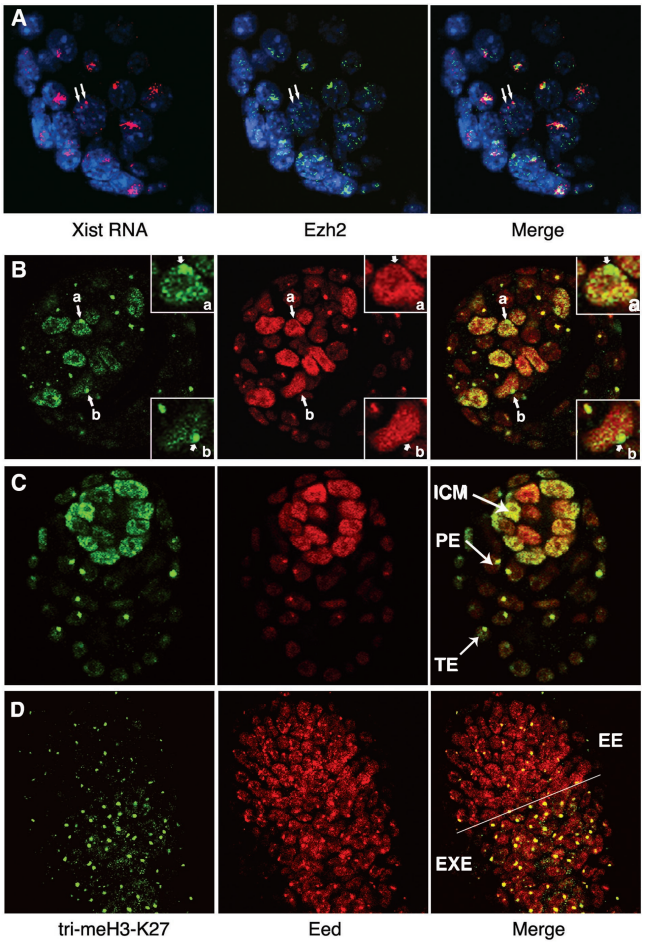

Fig. 3. Reactivation of Xp during ICM maturation. (**A**) Single optical section of ICM region of early XX blastocyst illustrating immunoRNA-FISH detection of *Xist* RNA (red) and Ezh2 (green). Counterstained with 4′,6′-diamidino-2-phenylindole (DAPI) (blue). Arrows indicate an example of a single cell where *Xist* RNA has been down-regulated [appearance of two pinpoint *Xist* RNA signals (*6*)] as well as the absence of Ezh2 localization. (**B**) Optical section through a mid-stage XX blastocyst, highlighting two cells (shown by arrows a and b; insets, expanded view), where Eed (red) foci are absent but tri-meH3-K27 (green) on Xi is still detectable. (**C**) Optical section through a mature (4.5 dpc) XX blastocyst illustrating that ICM cells have high Eed and meH3-K27 levels but no Xi foci. (**D**) Single optical section through a 5.5-dpc XX embryo illustrating reappearance of tri-meH3-K27 and Eed foci in the embryonic ectoderm region (EE), where random X inactivation is being initiated. Strong foci are seen in the extraembryonic ectoderm (EXE), where imprinted X inactivation has been maintained.

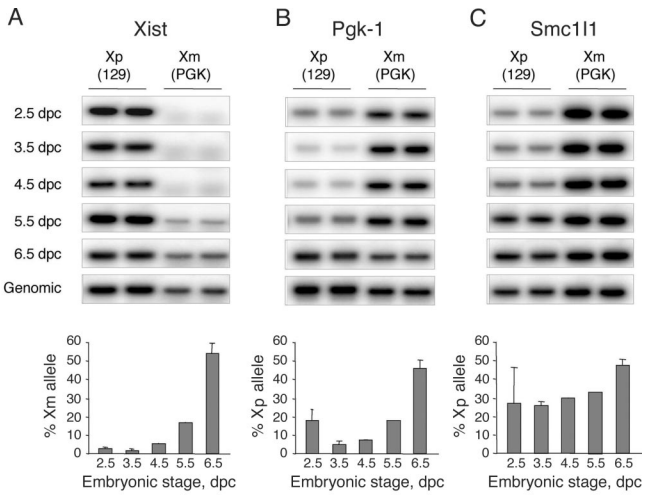

Fig. 4. Gene expression in early embryogenesis. Quantitative allelic expression assays for embryo stages from 2.5 to 6.5 dpc for (**A**) *Xist*, (**B**) *Pgk-1*, and (**C**) *Smc1l1*. The 3.5- to 6.5-dpc samples were from sexed (XX) embryos. Samplese from 6.5 dpc represent embryonic ectoderm regions of individual XX embryos. Examples show duplicate loadings of Xp (129) and Xm (PGK) alleles for each stage (129 denotes generic *Mus musculus domesticus*). Single nucleotide primer extension (SNuPE) analysis of polymerase chain reaction products from PGK × 129 F_1 genomic DNA (genomic) was used to normalize the data. Graphs illustrate mean values (± standard deviation where applicable) for % of Xm (*Xist*) or Xp (*Pgk-1 and Smc1l1*) transcripts obtained from a number of independent experiments (table S1). For control samples (6.5-dpc embryonic ectoderm and genomic DNA), Xm and Xp notation does not apply.

In light of evidence that chromosome-wide features of X inactivation are established in all cells of early embryos, we were interested to investigate allelic expression of individual X-linked genes. Embryos were obtained from crosses between *Mus musculus domesticus* and PGK strains, providing expressed single-nucleotide polymorphisms for quantitative allele specific assays (*16*). For early blastocyst and subsequent stages, XX and XY embryo pools were separated using a green fluorescent protein (GFP) transgene inherited on the paternal X chromosome (fig. S3A).

We first analyzed *Xist*, which is expressed only from Xi. Consistent with previous studies, expression was exclusively from Xp during preimplantation development, with up-regulation of the Xm allele first detectable at the onset of random X inactivation at 5.5 to 6.5 dpc (Fig. 4A).

We then analyzed expression of the *Pgk-1* gene (Fig. 4B), which is known to be subject to X inactivation, and also the *Smc1l1* gene (Fig. 4C), which is located at the distal end of the X chromosome and is also subject to X inactivation (Fig. S3B). At 2.5 dpc (eight-cell to early morula stage), both genes were biallelically expressed, consistent with activity of Xp. However, Xp transcript levels were relatively low, particularly at the *Pgk-1* locus. (In part, this may relate to the fact that both male and female embryos were included in the 2.5 dpc pool.) At 3.5 and 4.5 dpc (blastocyst stage), Xp *Pgk-1* levels were further reduced to approximately 5%, whereas levels of *Smc1l1* were relatively unchanged. In postimplantation embryos, Xp transcript levels increased again, and in embryonic ectoderm of 6.5 dpc XX embryos (after the onset of random X inactivation), the ratios of Xp and Xm alleles are essentially equivalent.

Analysis of the *Pgk-1* locus indicates inactivation of Xp begins as early as the eight-cell stage. The further marked reduction in Xp *Pgk-1* RNA at the early blastocyst stage is consistent with inactivation occurring in all cells, as indicated by our analysis with chromosome-wide markers. In contrast, the *Smc1l1* gene shows only partial X inactivation at the blastocyst stage, suggesting that the rate of X inactivation for individual genes may vary across the chromosome. Similar results, analyzing *Pgk-1* and other X-linked loci, have been reported in previous studies (*2*, *17*), leading to the idea that there may be a gradient of X inactivation in early embryos, centered on the *Xist* locus.

In summary, our results demonstrate that imprinted X inactivation of the paternal X chromosome, assayed at the level of chromosome-wide histone modifications and also repression of at least some loci, occurs in all cells of early mouse embryos, and that it is then reversed selectively in ICM cells after extinction of Xp *Xist* RNA expression. This latter observation indicates that heritability of X inactivation in early embryos requires ongoing *Xist* RNA ex-

pression, unlike XX somatic cells in which loss of *Xist* has little or no effect (*14*, *15*). Reversible *Xist*-dependent silencing has also been reported to occur in response to inducible *Xist* transgene expression in undifferentiated ES cells (*18*). Thus, our findings provide an in vivo corollary for this observation.

Reversibility of facultative heterochromatin in early embryos and ES cells is mirrored in the capacity of these cell types to reactivate the X chromosome in a somatic cell nucleus in ES cell fusion hybrids (*19*) or after nuclear transfer (*20*). Indeed, our results help to understand these findings. First, repression of Xp *Xist* occurs specifically in Nanog-positive cells at the time they are first allocated, suggesting that this is a property inherent to the pluripotent ICM lineage. The same activity in ES cells could result in repression of the somatic Xi *Xist* allele in ES-somatic cell hybrids. This then would lead to X reactivation in the ES nuclear environment, where heritability of X inactivation is strictly *Xist*-dependent. In the case of nuclear transfer, the Xi from the donor somatic cell is also the Xi in TE and PE lineages, but random X inactivation occurs in the embryo proper (*20*). This would be explained again if repression of *Xist* occurs specifically in ICM cells. TE and PE lineages would inactivate in response to maintained expression of the somatic Xi *Xist* allele, whereas ICM cells would repress *Xist*, establishing the ground state for random X inactivation in the embryo proper.

References and Notes

1. C. J. Epstein, S. Smith, B. Travis, G. Tucker, *Nature* **274**, 500 (1978).
2. J. Singer-Sam, V. Chapman, J. M. LeBon, A. D. Riggs, *Proc. Natl. Acad. Sci. U.S.A.* **89**, 10469 (1992).
3. N. Takagi, N. Wake, M. Sasaki, *Cytogenet. Cell Genet.* **20**, 240 (1978).
4. M. Monk, M. I. Harper, *Nature* **281**, 311 (1979).
5. R. L. Gardner, M. F. Lyon, *Nature* **231**, 385 (1971).
6. S. A. Sheardown *et al.*, *Cell* **91**, 99 (1997).
7. T. B. Nesterova, S. C. Barton, M. A. Surani, N. Brockdorff, *Dev. Biol.* **235**, 343 (2001).
8. J. Silva *et al.*, *Dev. Cell* **4**, 481 (2003).
9. K. Mitsui *et al.*, *Cell* **113**, 631 (2003).
10. I. Chambers *et al.*, *Cell* **113**, 643 (2003).
11. E. Heard *et al.*, *Cell* **107**, 727 (2001).
12. J. E. Mermoud, B. Popova, A. H. F. M. Peters, T. Jenuwein, N. Brockdorff, *Curr. Biol.* **12**, 247 (2002).
13. A. M. Keohane, L. P. O'Neill, N. D. Belyaev, J. S. Lavender, B. M. Turner, *Dev. Biol.* **180**, 618 (1996).
14. C. J. Brown, H. F. Willard, *Nature* **368**, 154 (1994).
15. G. Csankovszki, B. Panning, B. Bates, J. R. Pehrson, R Jaenisch, *Nature Genet.* **22**, 323 (1999).
16. Materials and Methods are available as supporting material on *Science* Online..
17. K. E. Latham, L Rambhatla, *Dev. Genet.* **17**, 212 (1995).
18. A. Wutz, R. Jaenisch, *Mol. Cell* **5**, 695 (2000).
19. M. Tada, Y. Takahama, K. Abe, T. Tada, *Curr. Biol.* **11**, 1553 (2001).
20. K. Eggan *et al.*, *Science* **290**, 1518 (2000).

21. We thank colleagues for helpful discussions and T. Jenuwein for kindly providing antisera. This work was supported by the Medical Research Council, UK.

Supporting Online Material

www.sciencemag.org/cgi/content/full/303/5658/666/DC1
Materials and Methods
Figs. S1 to S3
Table S1
References

17 October 2003; accepted 29 December 2003

Heterochromatic Silencing and HP1 Localization in *Drosophila* Are Dependent on the RNAi Machinery

Manika Pal-Bhadra,[1,3]* Boris A. Leibovitch,[2]* Sumit G. Gandhi,[3] Madhusudana Rao,[3] Utpal Bhadra,[1,3]† James A. Birchler,[1]† Sarah C. R. Elgin[2]†

Genes normally resident in euchromatic domains are silenced when packaged into heterochromatin, as exemplified in *Drosophila melanogaster* by position effect variegation (PEV). Loss-of-function mutations resulting in suppression of PEV have identified critical components of heterochromatin, including proteins HP1, HP2, and histone H3 lysine 9 methyltransferase. Here, we demonstrate that this silencing is dependent on the RNA interference machinery, using tandem *mini-white* arrays and *white* transgenes in heterochromatin to show loss of silencing as a result of mutations in *piwi*, *aubergine*, or *spindle-E* (*homeless*), which encode RNAi components. These mutations result in reduction of H3 Lys^9 methylation and delocalization of HP1 and HP2, most dramatically in *spindle-E* mutants.

Small RNA molecules have been found to play multiple roles in regulating gene expression. These include targeted degradation of mRNAs by small interfering RNAs (siRNAs) (posttranscriptional gene silencing, PTGS) (*1*, *2*), developmentally regulated sequence-specific translational repression of mRNA by micro-RNAs (miRNAs) (*3*), and targeted transcriptional gene silencing (TGS) (*4*–*9*). RNAi activity limits transposon mobilization and provides an antiviral defense (*10*). Recent work demonstrated that RNA interference (RNAi) is required to establish silencing at heterochromatic domains in fission yeast (*8*, *9*); appearance of transcripts from centromeric repeats is accompanied by loss of histone H3 Lys^9 methylation (*8*, *9*).

Many components of the RNAi machinery have been identified in *Drosophila melanogaster*, where they have been implicated in PTGS of the tandemly repeated *Stellate* genes, several retrotransposons, and *Alcohol dehydrogenase* (*Adh*) transgenes (*5*, *11*, *12*). Mutations in *aubergine* (*aub*), encoding a PAZ domain/

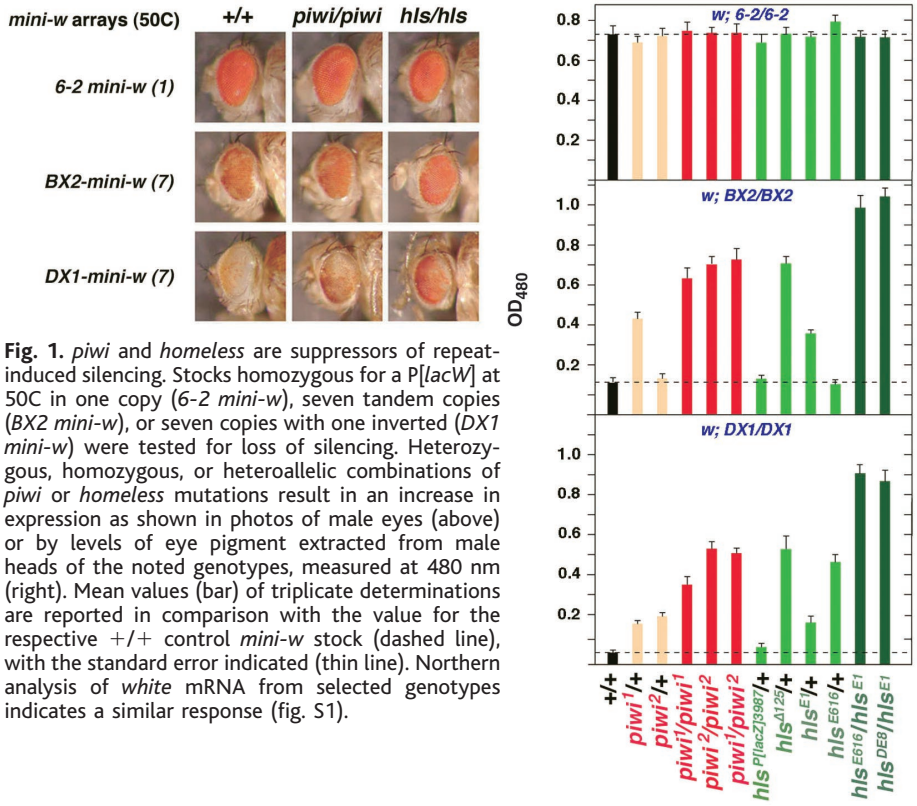

Fig. 1. *piwi* and *homeless* are suppressors of repeat-induced silencing. Stocks homozygous for a P[*lacW*] at 50C in one copy (*6-2 mini-w*), seven tandem copies (*BX2 mini-w*), or seven copies with one inverted (*DX1 mini-w*) were tested for loss of silencing. Heterozygous, homozygous, or heteroallelic combinations of *piwi* or *homeless* mutations result in an increase in expression as shown in photos of male eyes (above) or by levels of eye pigment extracted from male heads of the noted genotypes, measured at 480 nm (right). Mean values (bar) of triplicate determinations are reported in comparison with the value for the respective +/+ control *mini-w* stock (dashed line), with the standard error indicated (thin line). Northern analysis of *white* mRNA from selected genotypes indicates a similar response (fig. S1).